Available free online at www.medjchem.com

Mediterranean Journal of Chemistry

Mediterranean Journal of Chemistry **2022**, 12(1), 51-66

Design, synthesis, and characterization of hole transport materials for perovskite solar cells

Benjamin Brandes, Björn A. Weber and René Csuk *

Full Address: Martin-Luther-University Halle-Wittenberg, Organic Chemistry, Kurt-Mothes-Str. 2, D-06120 Halle (Saale), Germany

Abstract: Perovskite solar cells (PSC) are one of the most promising emerging photovoltaic technologies for a sustainable and profitable energy economy. However, finding alternative, stable, and cheap hole transport materials (HTM) required for these devices is one of the bottlenecks alongside finding optimal manufacturing processes to increase the market viability further. Here we show the synthesis and characterization of six small conjugated molecules HTMs and discuss their viability for future applications. For further validation, DFT calculations were carried out to underline the usability of the HTMs. In the future, these HTMs might help build cheaper and more efficient PSCs. Additionally, this work offers an insight on how to evaluate HTMs without needing to assemble a PSC. Finally, this work might help boost research efforts also for research groups with limited instrument availability.

Keywords: Hole Transport Material (HTM); Perovskite Solar Cell (PSC); Synthesis and Characterization, Energy Level Alignment.

1. Introduction

The growing demand for sustainable and reliable energy sources is prospering the research on photovoltaics (PV). The photovoltaic sensitizing effect of perovskite was firstly reported [1] in 2009, and the first certified Perovskite solar cells (PSCs) emerged [2] only a couple of years later. Nowadays, for some of them, an outstanding performance has been reported [2,3] holding a certified power conversion efficiency (PCE) of up to 25.7%. However, using lead-based perovskites causes a toxicity problem; thus, research in the field of alternatives is flourishing to find more eco-friendly systems [4,5]. PSCs are also frequently used in tandem solar cells because of their complementing absorption spectra. The concept for these cells originates from dye-sensitized solar cells (DSSCs), but they differ in structure, efficiency, and stability issues. A hole transport material (HTM) is used to extract the holes generated in the perovskite absorption layer. Replacing the well-established HTM spiro-OMeTAD, being much more often used in combination with an additional dopant, is believed to be the most promising attempt [6-8] to boost both stability and cost efficiency of the cells but also to improve the environmental impact of PSCs. To be competitive in the market, PSCs life spans > 20 years and PCE of 18% are needed (assuming HTM costs 78 $/g). Spiro-OMeTAD, however, is only commercially available [9] in Europe from European vendors (for example, Merck-Sigma-Aldrich or abcr GmbH) for > 210 $/g (typical lab quantities). Therefore, developing dopant-free HTMs to be used in PSCs is still the focus of scientific interest. However, polymeric HTMs like PTAA [poly(triaryl)amine] and P3HT [poly(3-hexylthiophene)] were successfully used in high-performance and more thermostable PSCs but suffered from batch-to-batch inconsistency and higher costs [10]. Moreover, developing suitable HTMs seems to be the bottleneck of perovskite solar cell modules [11] and thus for their worldwide commercialization. Herein we report the synthesis and characterization of chemically and optically stable small molecule HTMs, and their potential is discussed.

2. Results and Discussion

2.1. Design and synthesis

For the HTMs five core structures were chosen (Figure 1): hexaphenylbenzene (**1**), tetraphenylmethane (**4**), tetraphenylethene (**10**), spirobifluorene (**16**), and fluorene (**21**). Most of these are common structures in small molecule HTMs; most of these compounds can be obtained from local suppliers [12] at a reasonable price since they are already produced in large batches. For efficient hole transport, the morphology of the HTM is a vital parameter

*Corresponding author: René Csuk
Email address: rene.csuk@chemie.uni-halle.de
DOI: http://dx.doi.org/10.13171/mjc02206111628csuk

Received April13, 2022
Accepted May 10, 2022
Published June 11, 2022

strongly affected by π-π stacking and solid-state interactions. Thus, HTMs **3**, **6**, **12**, **19**, **20**, and **23** were chosen as promising candidates and thus synthesized (Figure 1).

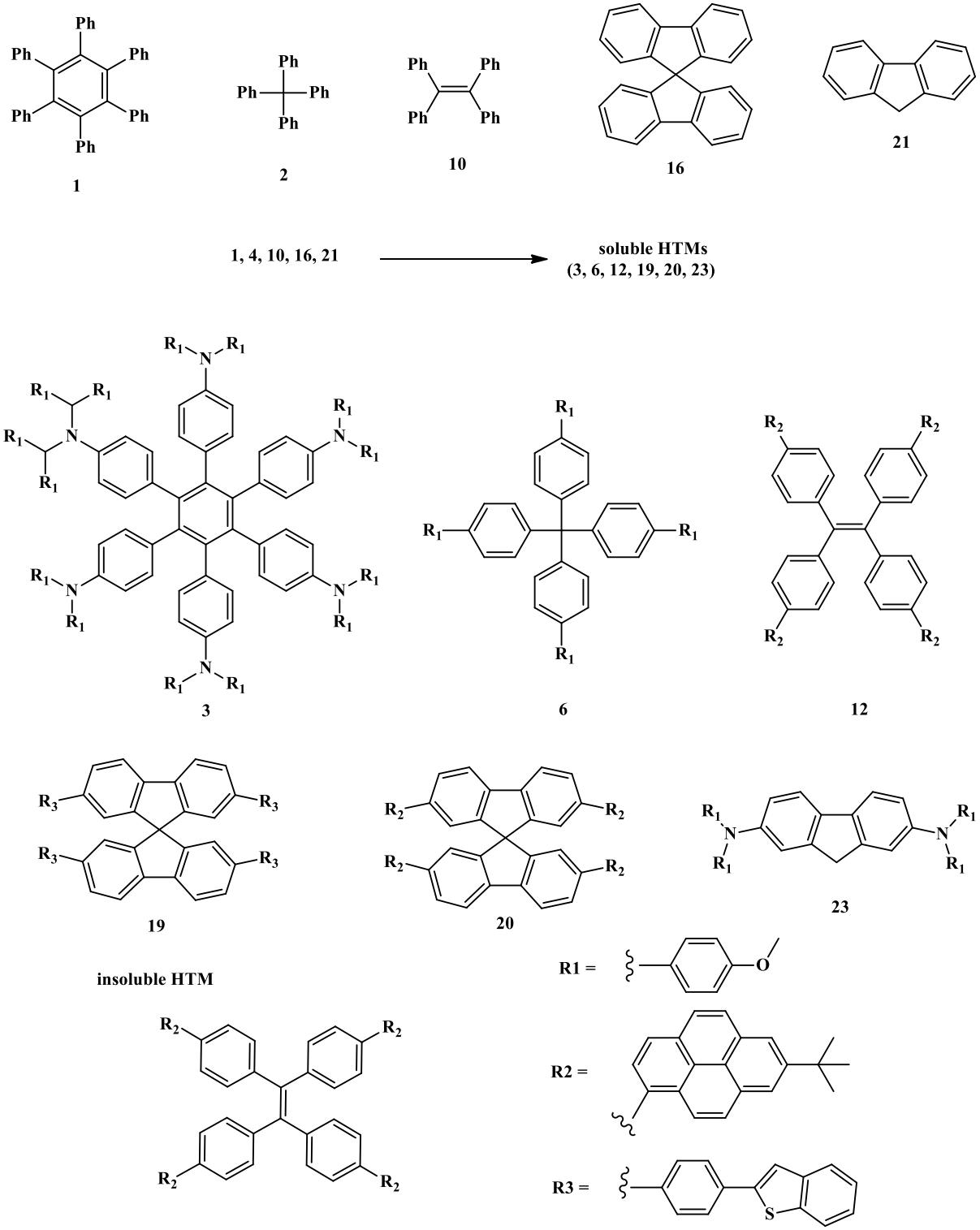

Figure 1. Core structures of the synthesized HTMs. HTMs **3**, **6**, **12**, **19**, **20**, and **23** were soluble in common solvents for aromatic compounds (for example DCM, $CHCl_3$, chlorobenzene, and toluene)

Their straightforward synthesis started from **1** as a commercially available starting material; the reaction sequence included a bromination reaction (→ 2) followed by a *Buchwald-Hartwig* reaction to yield HTM **3** in a total yield of 79% (Scheme 1). This sequence proved more convenient than other syntheses, and the costs per gram (21.03 $/g) depend strongly on the expenses of **1** [13,14].

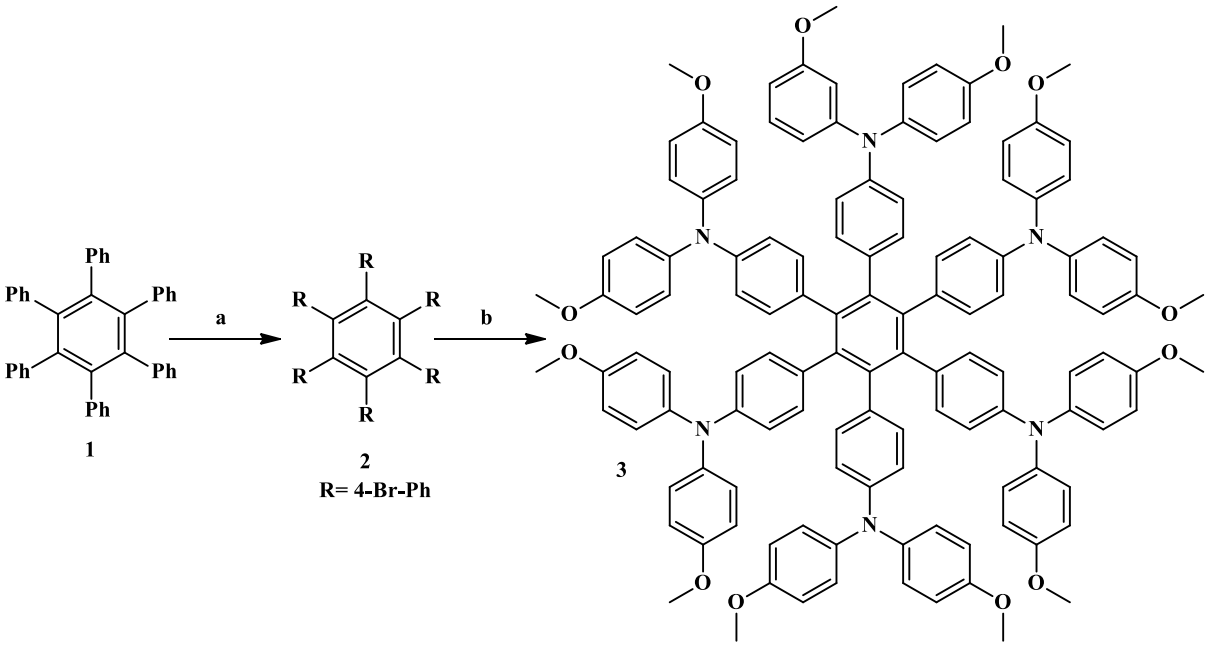

Scheme 1. Synthesis of HTM **3**: a) Br_2, RT, 50 min, 97% → EtOH, -20°C → RT, 6 h; b) t-BuOK, toluene, 0°C, 15 min → 4,4'-dimethoxydiphenylamine, $Pd(t\text{-}Bu_3P)_2$, toluene, RT → 111 °C, 24 h, 81%

The synthetic costs were calculated using assumptions adapted from literature and can be found for every compound in the supporting material [12]. Following the same synthetic scheme route for the synthesis of HTM **3**, HTM **6** was obtained in three steps with a total yield of 78%; other procedures [15] failed to deliver higher yields (Scheme 2).

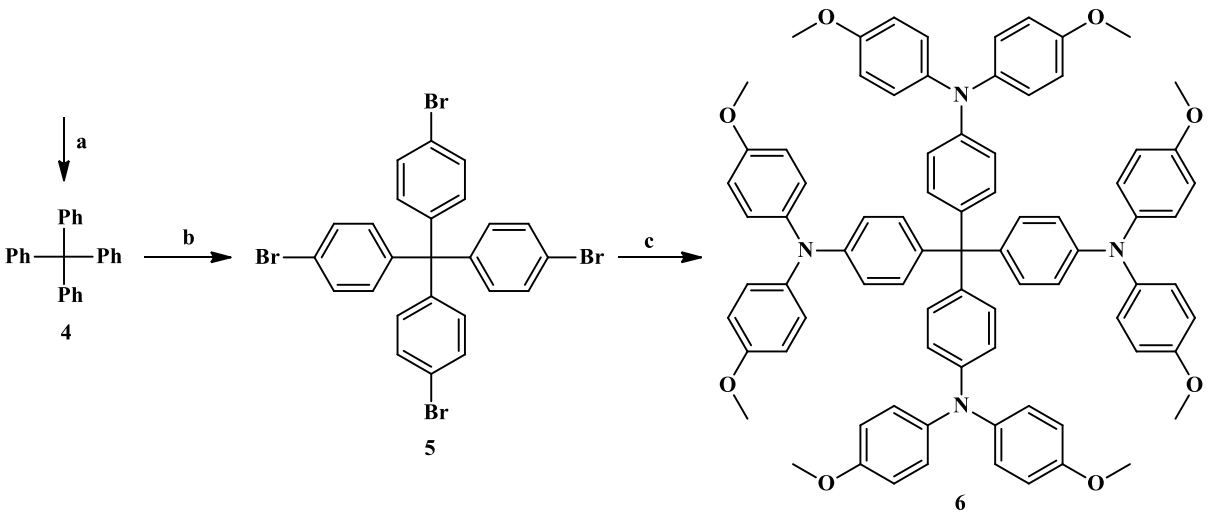

Scheme 2. Synthesis of **6**: a) aniline, triphenylchloromethane, 190°C, 15 min → HCl (2 M), MeOH, 80°C, 30 min → conc. H_2SO_4, isopentyl nitrite, -15°C, 1 h → hypophosphorous acid (50%), 50 °C, 87%; b) Br_2, RT, 20 min → EtOH, - 78 °C, 94%; c) t-BuOK, toluene, 0°C, 15 min → 4,4'-dimethoxydiphenylamine, $Pd(t\text{-}Bu_3P)_2$, toluene, RT → 111°C, 16 h, 95%

However, a different cross-coupling route was called for synthesizing HTM **12**. Firstly, the boronic acid pinacol ester **9** was synthesized by *Friedel-Crafts* alkylation, followed by bromination and lithiation-borylation, summing up to a total yield of 56%. Furthermore, the brominated core structure **11** was synthesized from benzophenone via a *McMurry* coupling reaction and a subsequent bromination yielding **11** in a total yield of 93%. In addition, a fourfold *Suzuki-Miyaura* reaction gave **12** in a diminished but acceptable total yield of 15% (Scheme 3).

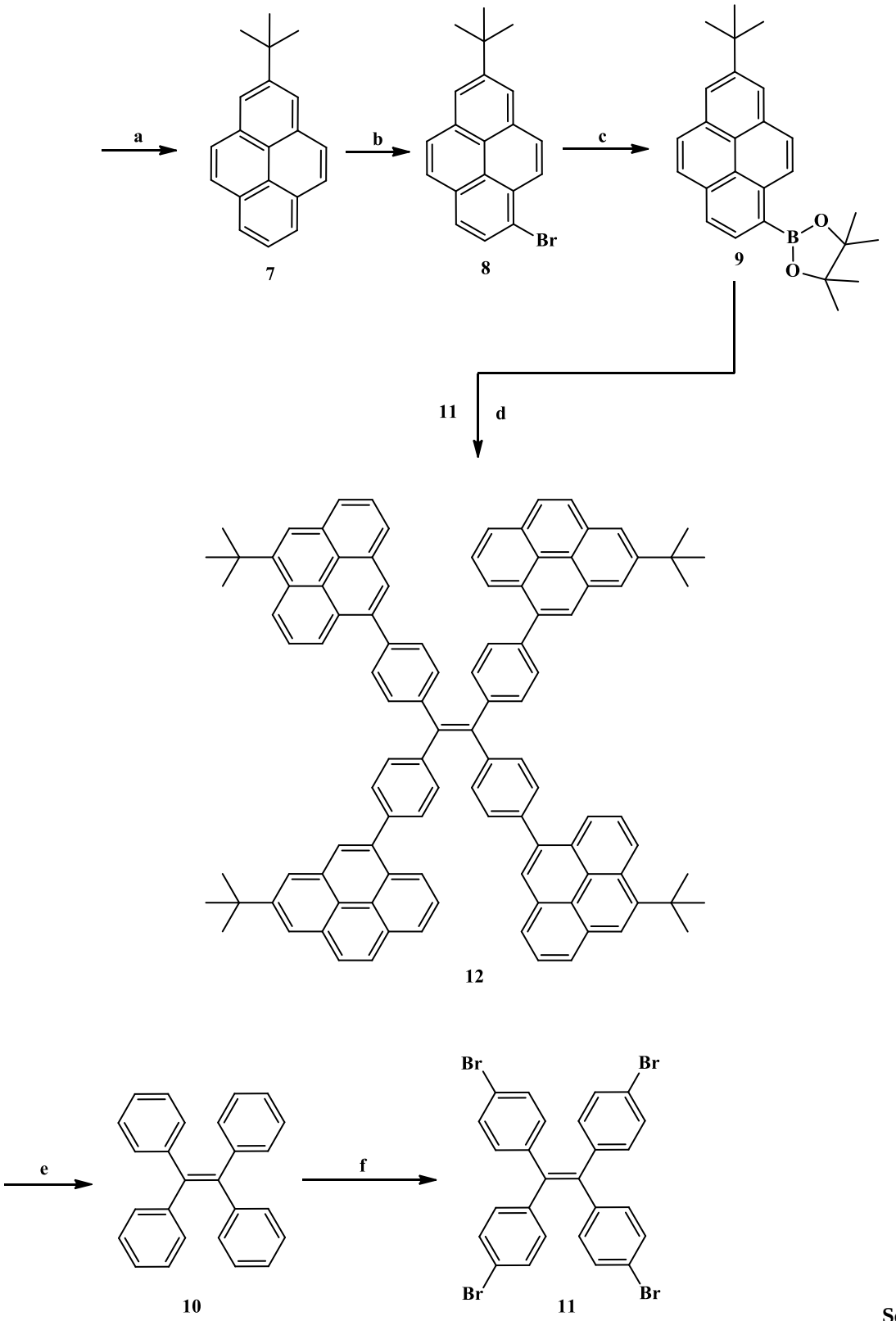

Scheme 3.

Synthesis of HTM **12**: a) pyrene, t-BuCl, $AlCl_3$, DCM, 0°C, 1 h, 80% → RT, 12 h; b) HBR (47%), H_2O_2 (30%), Et_2O/MeOH, 0°C → RT, 12 h, 83%; c) *n*-BuLi, THF, -78°C, 2 h → 2-isopropoxy-4,4,5,5-tetramethyl-1,3,2-dioxaborolane, - 78°C → RT, 12 h, 84%; d) $P(t\text{-}Bu)_3$, $Pd(OAc)_2$, K_2CO_3, toluene/H_2O, reflux, 33 h, 15%; e) $TiCl_4$, zinc, THF, -40°C → 90°C, 2 h → benzophenone, 0°C → 90°C, 12 h, 98%.; f) $FeCl_3$, Br_2, $CHCl_3$, RT, 12 h., 95%

For the synthesis of HTMs **19** and **20**, the brominated spirobifluorene **18** was synthesized in four steps with a total yield of 53%. In contrast, boronic acid pinacol ester **14** was synthesized by a *Suzuki-Miyaura* reaction with a total yield of 50%. The fourfold *Suzuki-Miyaura* reaction of **14** with **11** yielded an

insoluble product that could only be characterized by IR (ATR); its solubility was too low even for measurements by NMR. Furthermore, HTM **19** was accessed with a yield of 13%; this compound was soluble and thus characterized in full. Again, a fourfold *Suzuki-Miyaura* reaction between **9** and **18** was used to obtain HTM **20** with a total yield of 20% (Scheme 4).

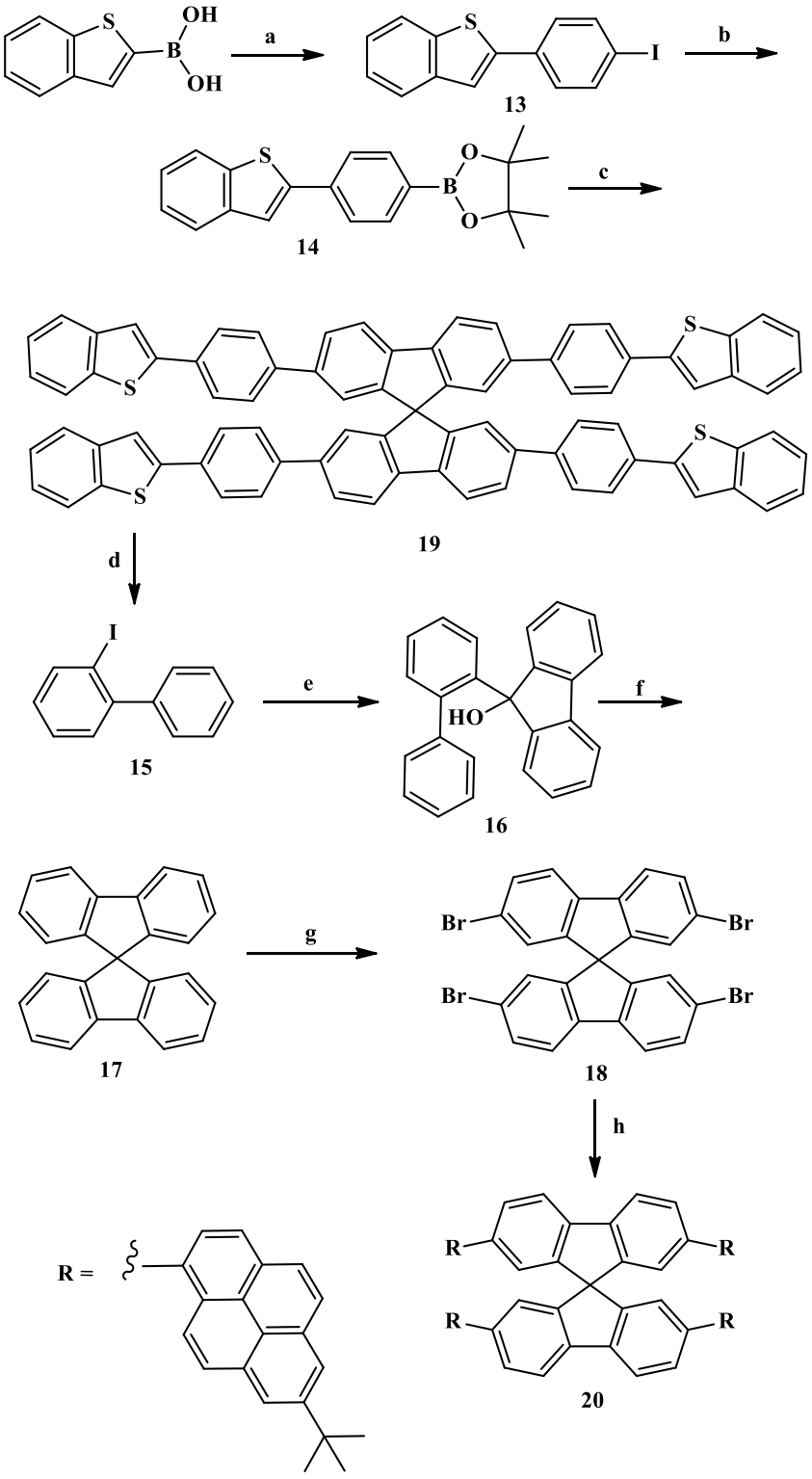

Scheme 4. Synthesis of HTM **19** and **20**: a) 4-bromo-1-iodobenzene, $P(t\text{-}Bu)_3$, $Pd(OAc)_2$, K_2CO_3, toluene, reflux, 10 h, 69%; b) n-BuLi, THF, -78°C, 2 h → 2-isopropoxy-4,4,5,5-tetramethyl-1,3,2-dioxaborolane, - 78°C → RT, 12 h, 72%; c) $P(t\text{-}Bu)_3$, $Pd(OAc)_2$, K_2CO_3, toluene/H_2O, reflux, 38 h, 23%; d) 2-aminobiphenyl, conc. HCl, H_2O, RT → $NaNO_2$, 0°C, 45 min → KI, 0 °C,→ RT, 12 h, 71%; e) t-BuLi, Et_2O, -78 °C, 1 h → fluorenone, -78°C, 45 min → RT, 1 h, 87%; f) HCl, AcOH, reflux, 30 min, 95%; g) $FeCl_3$, Br_2, $CHCl_3$, 0°C → RT, 3 h → cyclohexene, RT, 1 h, 90%; h) **9**, $P(t\text{-}Bu)_3$, $Pd(OAc)_2$, K_2CO_3, toluene/H_2O, reflux, 31 h, 20%

To investigate HTMs of smaller molecular size, fluorene (**21**) was brominated and used as a starting material in a *Buchwald-Hartwig* reaction to obtain HTM **23** with a total yield of 69% (Scheme 5).

Thus, most of the HTMs' precursors procedures were found that give good to excellent yields; all of them were optimized to provide easy workup procedures for future industrial use, thus focusing on easy recrystallization rather than purification procedures based on chromatography except for those HTMs that were obtained from *Suzuki-Miyaura* reactions.

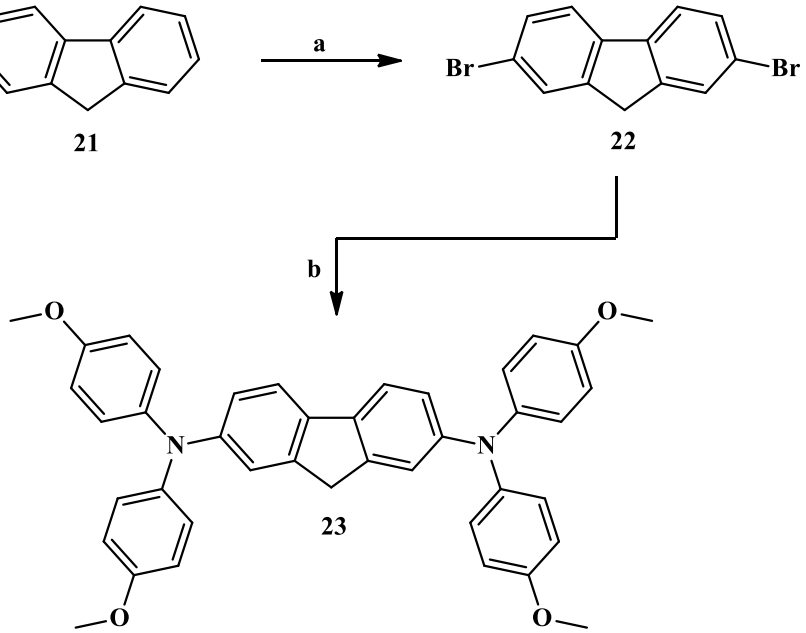

Scheme 5. Synthesis of HTM **23**: a) Br_2, $FeBr_3$, $CHCl_3$, in the dark, 0°C → RT, 3 h, 89%; b) 4,4'-dimethoxydiphenylamine, t-BuONa, $Pd(OAc)_2$, t-Bu_3P, toluene, RT → 111 °C, 12 h., 78%

During the latter reactions, many by-products were formed, including boronic ester dimerization products but also not fully reacted brominated core structures. However, this obstacle can be avoided by adding the boronic esters in smaller batches and optimizing the trans-metalation reaction by optimizing the polarity of the reaction [16] or synthesizing iodinated core structures instead of brominated compounds. We refrain from a full estimation of the costs for all the HTMs due to the cost-diminishing effect of upscaling and costs of reagents, catalysts, and solvents depending both on their respective point of sale and quantity.

2.2. DFT calculations

Time-dependent density functional theory (TD-DFT) was used to get some insights into the electrical behavior of the synthesized HTMs. These TD-DFT calculations involved a standard Becke-three-Lee-Yang-Parr (B3LYP) hybrid functionalization based on optimized geometries with basis sets 6-31g(d,2p), 6-311g(d,p), and cc-pvtz. Carrier transport in organic semiconductors preferentially occurs in the highest occupied molecule orbital (HOMO) for holes and the lowest unoccupied molecule orbital (LUMO) for electrons. Therefore, a well-spread delocalization of orbitals and high dipole moments are favorable for charge transport and hole transfer integral to provide a good hole transport [17]. Thus, visualization of the HOMOs (Figure 2) and the calculated dipole moments give information on these parameters and can be used to discuss electronical donor and acceptor mechanisms.

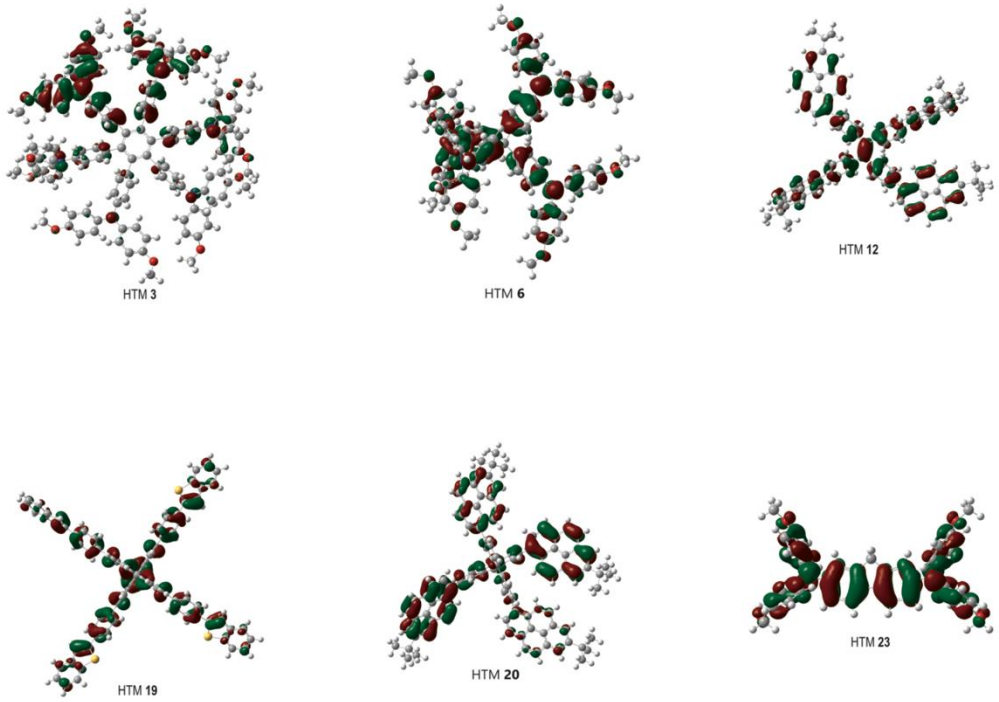

Figure 2. Visualization of the HTM's HOMO and the calculated dipole moments: HTM **3**: 4.84 D, HTM **6**: 2.78 D, HTM **12**: 1.23 D, HTM **19**: 0.89 D; HTM **20**: 1.01 D; HTM **23**: 3.69 D

As a result, the tert. butyl groups of the pyrene-based HTMs **12** and **20** are not involved in the HOMO and the LUMO, and the methoxy groups of HTMs **3** and **6** could be helpful for perovskite anchoring and an inhibition of dimerization. The absence of large orbitals in the benzene unit of the benzo[*b*]thiophene could also benefit HTM **19**. The most polar HTM seems to be HTM **3,** which holds a calculated dipole moment of 4.84 D while HTM **19** showed the lowest dipole moment of 0.89 D.

As typical for DFT calculations, the calculated HOMOs of the HTMs are to be regarded as being systematically underestimated in the same order as the obtained HOMOs obtained from cyclic voltammetry (CV) experiments (Table 1). Interestingly, the calculated singlet excitations for the isolated state of the HTMS were in excellent agreement with the 0-0 transitions obtained from combined UV-Vis and excitation spectra.

2.2. 2.3. Electrophysical and thermal properties

The energy level alignment (ELA) is one of the most important parameters of HTMs [17]. Cyclic voltammograms and emission spectroscopy experiments were carried out to determine the energy levels. The supplementary materials file depicts cyclic voltammograms and emission spectra of HTMs. The HTMs **3, 6**, **12**, **19**, **20,** and **23** showed quasi-reversible shape behavior in the limited scan window, while the onset potential used for calculation did not change significantly at lower scan rates. The HTMS 6, 12, 19, and 20 seem to be suitable for a n-i-p device setup if $MAPbBr_3$ was used [18], while HTMs **3** and **23** showed good ELA with a p-i-n device setup if $MAPbI_3$ was used (Figure 3) [19]. All HTMs offered sufficient electron blocking capability due to a higher electron affinity (EA) than the conduction band of the perovskite.

Lifetime measurements of excited states showed less than 1 ns for all HTMs, which was the equipment's detection limit. Since the melting point and the glass-transition temperature (T_g) are important parameters of HTMs, DSC measurements were carried out to determine the thermal properties and stabilities. HTM **23** showed a very low T_g of 38.7°C, which makes it unsuitable for applications in PSCs, despite a proper ELA. In addition to the thermal instability, HTM **23** was soluble in DMSO, making it unusable for spin-coating applications. Despite these thermal and solubility issues, HTM **23** was used in a p-i-n device setup, which delivered an average PCE of 12.41 ± 0.66% [20]. Paralleling our investigations, another research group managed to build a PSC using HTM **3**, which showed to give just 0.7% less PCE than spiro-OMeTAD with an average PCE of 16.4% [14].

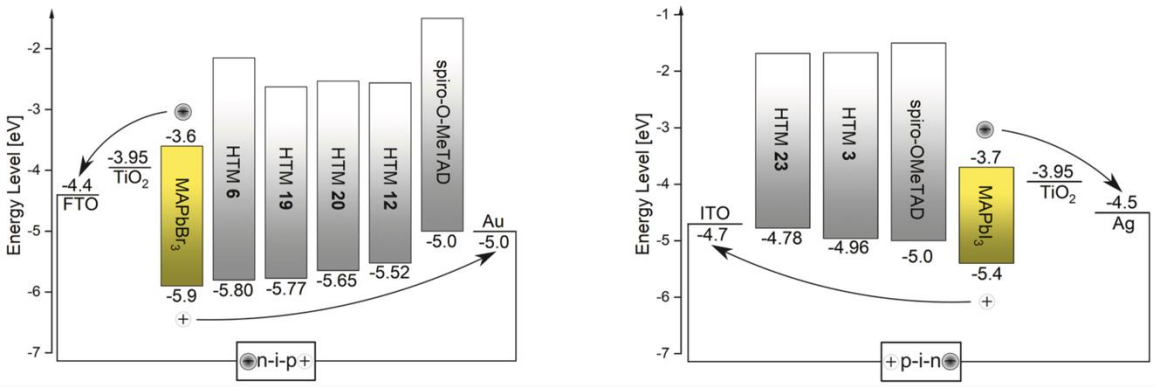

Figure 3. Possible n-i-p/p-i-n device structures for synthesized HTMs with ELA. Spiro-OMeTAD was used as a reference, while the respective perovskite was chosen because of their measured IE and EA as films on TiO_2

For good hole transport efficiencies, the Coulomb attraction between the electron-hole pair has to be overcome in the perovskite layer to separate positive and negative charges [21]. The charge separation energy is often called the transport gap E_T, which is different from the optical band gap E_{opt}, since the electron and hole in organic semiconductors are not on the same molecule [22]. Since CV experiments were taken in solution; the values differ from those obtained from UV photoelectron spectroscopy (UPS) measurements in solid-state because the solvation energy is usually higher than the polarization energy in bulk solids. A study about small organic semiconductor bandgaps showed E_T to be underestimated by 16% on average if electrochemical measurements were used to measure the electrochemical gap [23]. Thus, HOMO values taken from CV experiments are sometimes underestimated by a factor α^+ that can be used to calculate the better ionization energy : $I_C = \alpha^+ \times (eE_{ox}) + \beta^+$. While E_{ox} is the oxidation potential from CV, e represents the unit charge, and β^+ is (with 4.8 eV) the ferrocenium/ferrocene (Fc^+/Fc) vacuum level. Therefore, an empirical correction of the experimental data α^+ was assumed to be 1.16 (16% underestimation). In addition, calculating the LUMO from the reduction cycle of the CV experiments for the bandgap can be way off since the LUMO contains no extra electron. In this work, the LUMO was estimated from the sum of the HOMO and the 0-0 transition energy, defined as the intersection of the UV-Vis spectrum and the excitation spectrum in solution. Using the TAUC plot for optical band gap calculation is acceptable for inorganic semiconductors. For some HTMs, using the onset of the absorption maxima of the analyte (being dissolved in $CHCl_3$) also provides a good estimation [24]. In an empirical study by *J. Sworakowski* et al. [23] the average underestimation of the transport gap E_T using this technique was reported at 37% [15]. These results can be expressed as $E_T = E^{LUMO} - E^{HOMO} = 1.37 \times E_{opt}$. The empirically adjusted n-i-p/p-i-n setups (Figure 3) revealed that almost all HTMs are still viable in their ELA.

Table 1. Thermal and electronical properties of HTMs: a) 0-0 transition determined by the intersection of absorption and emission spectra taken in solution; b) determined by CV measurements about the (Fc^+/Fc) vacuum level (details in the experimental part); c) deduced from the addition of E_g (0-0) and the HOMO.

HTM	Melting point / (T_g)	Bandgap (E_g)[eV]			HOMO[b] [eV]	LUMO[c] [eV]	I_C [eV]	E_T [eV]
		0-0[a]	DFT	E_{opt}				
3	> 330 °C	3.29	3.25	3.24	-4.96	-1.67	-4.99	4.51
6	> 330 °C	3.65	3.58	3.52	-5.8	-2.15	-5.96	5.00
12	> 330 °C	2.96	2.9	3.08	-5.52	-2.56	-5.64	4.06
19	271.4 °C	3.15	3.08	3.1	-5.77	-2.63	-5.93	4.47
20	> 300 °C	3.12	3.12	3.07	-5.65	-2.53	-5.78	4.27
23	76 °C / (38.7 °C)	3.09	3.13	3.01	-4.78	-1.68	-4.77	4.24

It also has to be considered that band bending may occur with gradual deposition of the organic material, so HTMs **6** and **19** may still be able to transport holes to the gold anode. The actual positions of the energy levels probably lie between the observed and the empirically corrected values. In summary, each of our HTMs showed similar or even better electron blocking capabilities than spiro-OMeTAD.

3. Conclusion

A series of small molecule HTMs was synthesized, characterized, and discussed for future testing in PSCs. Nearly each synthesized HTM showed suitable ELA with selected perovskites and even better electron blocking capabilities than "gold standard" spiro-OMeTAD while being more non-polar and more stable against moisture. This makes them promising candidates for extended testing in assembled PSCs.

4. Experimental

NMR spectra were recorded using the Agilent spectrometers DD2 500 MHz, and VNMRS 400 MHz (δ given in ppm, J in Hz; typical experiments: APT, H-H-COSY, HMBC, HSQC, NOESY), MS spectra were taken on an Advion Expression CMS instrument. TLC was performed on silica gel (Macherey-Nagel, detection with cerium molybdate reagent); melting points were uncorrected (Leica hot stage microscope, or BUCHI melting point M-565), and elemental analyses were performed on a Foss-Heraeus Vario EL (CHNS) unit. IR spectra were recorded on a Perkin Elmer FT-IR spectrometer Spectrum 1000 or a Perkin-Elmer Spectrum Two (UATR Two Unit). Lifetime measurements were carried out with a Spectrofluorometer FS5 from EDINBURGH INSTRUMENTS using a picosecond pulsed light-emitting diode and degassed solutions of HTMs in $CHCl_3$. Emissions spectra were measured with a LS 50 B luminescence spectrometer from PERKIN ELMER. DSC measurements were performed with a DSC 8000 from PERKIN ELMER. Cyclic voltammetry was carried out with a compact potentiostat from METHROHM using an Ag/AgCl reference, glassy carbon, and a platinum electrode from eDAQ tetrabutylammonium hexafluoro-phosphate solution (0.1 M) in degassed DCM [25]. For reference, the analyte solution (2 mM) was measured with and without approximately the same amount of ferrocene at alternating scanning ranges (20/100/300 mV/s) and directions (+/-) [26-29]. The electronic window of the electrolyte was tested in advance, and the scanning directions were alternated with every new scan, which started at the open-circuit voltage. For the HOMO calculation, the formula: $HOMO\ [eV] = \left(eE_{ox\ (onset)}\right) + \beta^{+}$ was used with β^{+} being the ferrocenium/ferrocene vacuum level (4.8 eV). For this, the average onset potential calculated from the analyte ($E_{ox\ (onset)}$) from three scans was used, referencing the average ferrocene onset potential from three scans by subtraction. The solvents were dried according to usual procedures. Fresh distilled and degassed solvents and dried glassware were used for air-sensitive reactions. A combination of the Nova and Origin 2019 software was used for the calculations [30]. DFT calculations were executed with Gaussian 16 [31]. Costs were calculated by comparing and choosing the cheapest vendor prices per g of local European vendors.

4.1. General procedure (GP 1) for *Buchwald-Hartwig* reactions

To a solution of the aryl halide (**6**, **8**, **22**) in toluene (100 mL/mmol) under argon atmosphere was added *t*-BuOK, or *t*-BuONa at 0°C, and the solution was stirred at that temperature for another 15 min. The mixture was allowed to warm up to RT, and $Pd(t\text{-}Bu_3P)_2$ or $Pd(OAc)_2$ and P(t-Bu)$_3$ (5 mol%) were added. After adding the 4,4'-dimethoxydiphenylamine (1.7 eq), the reaction was stirred under reflux until TLC showed complete consumption of the amine.

Hexakis(4-bromophenyl)benzene (2)

The compound was prepared as described [32] For workup; the reaction mixture was cooled to -20°C. EtOH (40 mL) was added at that temperature, and the reaction was allowed to stir at RT for another 6 h. The reaction mixture was stored at -20°C for 16 h, and the precipitate was filtered off and washed with cold EtOH. Compound **2** (3.66 g, 97%, [19057-50-2]) was obtained as a white solid; m.p. >330°C (lit.:[32] >300 °C); R_F = 0.34 (*n*-hexane/ethyl acetate, 6:1);
IR (KBr): $\tilde{\nu}$ = 1636*m*, 1492*m*, 1391*w*, 1139*w*, 1072*m*, 1010*m*, 826*m*, 764*m*, 533*w*, 475*w* cm^{-1};
UV/vis ($CHCl_3$): λ_{max} (log ε) = 246 (4.33), 269 (4.45), 300 (4.16) nm;
^{1}H NMR (500 MHz, $CDCl_3$): δ = 7.44 (d, *J* = 8.4 Hz, 12H, 3-H), 6.96 (d, *J* = 8.4 Hz, 12H, 4-H) ppm;
^{13}C NMR (100 MHz, $CDCl_3$): δ =139.9 (C-1), 138.6 (C-2), 133.0 (C-4), 131.0 (C-3), 121.1 (C-5) ppm.

Hexakis[*N*,*N*-bis(4-methoxyphenyl)-4-aminophenyl]benzene (3)

Compound **3** was obtained by reacting **2** (1.0 g, 1 mmol) and *t*-BuOK (0.83 g, 7.4 mmol) using GP1. After 24 hours of heating the mixture under reflux, the solvent was evaporated at diminished pressure, the residue was taken up in DCM (8 mL) and added dropwise to ice-cold MeOH (160 mL); the solid was filtered off, and washed with MeOH to obtain compound **3** (1.53 g, 81%, [213553-59-4]) as a violet solid; m.p. >330°C; R_F = 0.15 ($CHCl_3$/MeOH, 9:1);
IR (KBr): $\tilde{\nu}$ = 2832*w*, 1606*w*, 1505*s*, 1463*w*, 1316*w*, 1239*s*, 1178*w*, 1105*w*, 1036*m*, 826*m*, 621*s*, 568*w* cm^{-1};
UV/vis ($CHCl_3$): λ_{max} (log ε) = 270 (4.24), 269 (4.74) nm;
^{1}H NMR (500 MHz, $CDCl_3$): δ = 6.93 (d, *J* = 8.9 Hz, 24H, 7-H), 6.77 (d, *J* = 9.0 Hz, 24H, 8-H), 6.68 (d, *J* = 8.7 Hz, 12H, 4-H), 6.63 (d, *J* = 8.6 Hz, 12H, 3-H), 3.75 (s, 36H, 10-H) ppm;
^{13}C NMR (100 MHz, $CDCl_3$): δ = 155.2 (C-9), 154.6 (C-5), 141.5 (C-6), 140.1 (C-1), 134.4 (C-2), 132.4 (C-4), 125.5 (C-7), 120.5 (C-3), 114.6 (C-8), 55.4 (C-3 + C-10) ppm;
MS (ESI, CH_2Cl_2): m/z = 949.00 (100%, $[M]^{2+}$), 1897.73 (14%, $[M]^{+}$).

Tetraphenylmethane (4)
Triphenylmethyl chloride (20.0 g, 71.1 mmol) and aniline (17.02 mL, 187 mmol) were stirred at 190°C for 15 min, cooled to RT, and the resulting solid was crushed. The solid was treated with HCl (2 M, 80 mL) in MeOH (120 mL), stirred at 80°C for 30 min, filtered off, washed with water, and air-dried. The dried solid was suspended in DMF (200 mL), the solution was cooled to -15°C, and treated with conc. H_2SO_4 (22 mL), and isopentyl nitrite (17 mL) were added dropwise. The reaction was stirred for 1 h, and hypophosphoric acid (50%, 36 mL) was added dropwise. The reaction was stirred at 50°C until gas evolution stopped. The solid was filtered off, washed with DMF, water, and EtOH followed by recrystallizing from DCM to yield compound **4** (17.3 g, 87%, [630-76-2]) [33] as colorless crystals; m.p. 279°C (lit.:[34] 236-238°C); R_F = 0.32 (hexane/DCM, 9.5:0.5);
IR (KBr): $\tilde{\nu}$ = 1636*w*, 1492*m*, 1441*w*, 1182*w*, 1081*w*, 1036*w*, 765*m*, 750*m*, 702*s*, 632*m* cm^{-1};
UV/vis ($CHCl_3$): λ_{max} (log ε) = 248 (4.13), 279 (3.64) nm;
^{1}H NMR (500 MHz, $CDCl_3$): δ = 7.28–7.17 (m, 20H, 3-H + 4-H + 5-H) ppm;
^{13}C NMR (100 MHz, $CDCl_3$): δ = 147.3 (C-2), 131.6 (C-3), 127.9 (C-4), 126.4 (C-5), 65.5 (C-1) ppm;
MS (APCI): m/z = 242.8 (100%, $[M\text{-}Ph]^+$).

Tetrakis(4-bromophenyl)methane (5)
To bromine (6.5 mL, 125 mmol) was added **4** (2.0 g, 6.4 mmol), and stirring at RT was continued for 20 min. The reaction mixture was cooled to -78°C, EtOH (17.5 mL) was added, and the reaction was allowed to warm up to RT. The precipitate was filtered off, washed with a saturated sodium thiosulfate solution and water. Subsequently, the dried solid was purified by column chromatography (SiO_2, hexane/DCM, 9.5:0.5) to obtain **5** (3.8 g, 94%, [105309-59-9]) as a white solid; m.p. >330°C (lit.:[34] > 300°C);R_F = 0.64 (hexane/DCM, 9.5:0.5);
IR (KBr): $\tilde{\nu}$ = 1636*w*, 1480*m*, 1396*w*, 1078*m*, 1009*s*, 809*m*, 532*w*, 510*w* cm^{-1};
UV/vis ($CHCl_3$): λ_{max} (log ε) = 248 (4.48), 289 (3.58) nm;
^{1}H NMR (500 MHz, $CDCl_3$): δ = 7.40 (d, *J* = 8.8 Hz, 8H, 4-H), 7.02 (d, *J* = 8.8 Hz, 8H, 3-H) ppm; ^{13}C NMR (100 MHz, $CDCl_3$): δ = 144.8 (C-2), 132.8 (C-3), 131.5 (C-4), 121.2 (C-5), 64.1 (C-1) ppm;
MS (APCI): m/z = 476.3 (100%, $[M\text{-}PhBr]^+$).

Tetrakis[*N*,*N*-bis(4-methoxyphenyl)-4-aminophenyl]methane (6)
Compound **5** was obtained by reacting **4** (1.0 g, 1.6 mmol) and *t*-BuOK (0.82 g, 7.3 mmol) following GP1. After 16 hours of heating the reaction mixture under reflux, the solvent was evaporated, the residue was re-dissolved in $CHCl_3$ (6 mL) and added dropwise to ice-cold MeOH (150 mL), filtered, washed with MeOH, and dried to obtain compound **3** (1.87 g, 95%, [362052-19-5]) as a violet solid; m.p. >330°C; R_F = 0.22 ($CHCl_3$/MeOH, 9:1);
IR (KBr): $\tilde{\nu}$ = 2834*m*, 1636*m*, 1504*s*, 1464*w*, 1318*w*, 1240*m*, 1036*w*, 825*w* cm^{-1};
UV/vis ($CHCl_3$): λ_{max} (log ε) = 337 (4.06) nm;
^{1}H NMR (500 MHz, $CDCl_3$): δ = 7.03 (d, *J* = 8.9 Hz, 16H, 7-H), 6.96 (d, *J* = 8.8 Hz, 8H, 4-H), 6.80 (d, *J* = 9,0 Hz, 16H, 8-H), 6.78 (d, *J* = 8.8 Hz, 8H, 3-H), 3.78 (s, 24H, 10-H) ppm;
^{13}C NMR (100 MHz, $CDCl_3$): δ = 155.8 (C-9), 146.4 (C-5), 141.3 (C-6), 139.6 (C-2), 131.8 (C-3), 126.6 (C-7), 119.2 (C-4), 114.8 (C-8), 55.6 (C-10) ppm;
MS (ESI, CH_2Cl_2): m/z = 614.27 (40%, $[M]^{2+}$), 1228.4 (100%, $[M]^{+}$).

2-*tert*-Butylpyrene (7)
Pyrene (6.0 g, 29.7 mmol) was dissolved in dry DCM (100 mL) under argon atmosphere. At 0°C, 2-chloro-2-methylpropane (3.22 mL, 29.7 mmol), and $AlCl_3$ (4.75 g, 35.6 mmol) were added under stirring. The reaction was stirred at that temperature for 1 h until the reaction turned red and stirring was continued at RT overnight. The reaction mixture was poured onto ice in a separation funnel and washed with a saturated sodium bicarbonate solution (50 mL). The aqueous phase was extracted with DCM (3 × 100 mL), and the organic phase was washed with water (100 mL), brine (100 mL), and dried over $MgSO_4$. Subsequently, the solvent was removed under reduced pressure, and the orange solid was recrystallized from minimal amounts of MeOH in a microwave reactor at 120°C to obtain **7** (6.16 g, 80%, [78751-62-9]) as white plates; m.p. 110°C (lit.:[35] 110–112°C); R_F = 0.5 (petroleum ether/DCM, 9:1);
IR (KBr): $\tilde{\nu}$ = 2961*s*, 1602*m*, 1461*w*, 1386*w*, 1356*w*, 1225*m*, 876*s*, 840*m*, 815*m*, 800*w*, 712*s* cm^{-1};
UV/vis ($CHCl_3$): λ_{max} (log ε) = 248 (4.4), 267 (4.08), 278 (4.24), 296 (3.55), 310 (3.72), 324 (4.09), 339 (4.3) nm;
^{1}H NMR (500 MHz, $CDCl_3$): δ = 8.27 (s, 2H, 14-H + 16-H), 8.18 (d, *J* = 7.6 Hz, 2H, 11-H + 13-H), 8.09 (m, 4H, 1-H + 2-H, 8-H + 9-H), 8.00 (t, *J* = 7.6 Hz, 1H, 12-H), 1.64 (*s*, 9H, 18-H_3) ppm;
^{13}C NMR (126 MHz, $CDCl_3$): δ = 149.0 (C-15), 131.0 (C-5), 131.0 (C-4), 127.6 (C-1 + C-9), 127.3 (C-2 + C8), 125.5 (C-12), 124.8 (C-11 + C-13), 124.7 (C-3 + C-7), 123.0 (C-6 + C-10), 122.2 (C-14 + C-16), 35.3 (C-15), 32.0 (C-18) ppm;
MS (ASAP): m/z = 359.0 (100%, $[M]^{+}$).

6-Bromo-2-(*tert*-butyl)pyrene (8)
Compound **7** (3.0 g, 11.6 mmol) was dissolved in Et_2O/MeOH (1:1, 60 mL), cooled to 0°C, and HBr (47% in H_2O, 1.48 mL, 12.8 mmol) was added. Then H_2O_2 (30% in H_2O, 1.19 mL, 11.6 mmol) was added dropwise during 5 min at 0°C. Once the solution turned red, the solution was allowed to warm to RT and stirred overnight. Subsequently, a saturated sodium bicarbonate solution (10 mL) was added, and the organic phase was separated. The aqueous phase was extracted with DCM (3 × 50 mL), while the combined organic phases were washed with water (50 mL), brine (50 mL), and dried over $MgSO_4$.The yellowish solid, obtained from removing the solvent,

was recrystallized from hexane in an microwave oven at 120°C to obtain **8** (3.24 g, 83%, [78751-74-3]); m.p. 157°C; R_F = 0.57 (petroleum ether/DCM, 9:1);
IR (KBr): $\tilde{\nu}$ = 2962*s*, 1627*m*, 1590*s*, 1475*m*, 1386*m*, 1360*m*, 1228*s*, 1159*m*, 1014*m*, 922*w*, 878*s*, 838*s*, 820*m*, 804*m*, 710*s* cm^{-1};
UV/vis ($CHCl_3$): λ_{max} (log ε) = 250 (3.9), 271 (3.56), 283 (3.74), 304 (2.93), 318 (3.29), 332 (3.7), 349 (3.9) nm;
^{1}H NMR (500 MHz, $CDCl_3$): δ = 8.39 (d, *J* = 9.2 Hz, 1H, 2-H), 8,27 (d, *J* = 1.6 Hz, 1H, 16-H), 8.26 (d, *J* = 1.6 Hz, 1H, 14-H) 8.18 (d, *J* = 8.2 Hz, 13-H), 8.15 (d, *J* = 9.1 Hz, 1H, 1-H), 8.06 (d, *J* = 8.9 Hz, 1H, 9-H), 7.98 (d, *J* = 9.0 Hz, 1H, 12-H), 7.96 (d, *J* = 8.2 Hz, 1H, 8-H), 1.60 (s, 9H, 18-H_3) ppm;
^{13}C NMR (126 MHz, $CDCl_3$): δ = 149.9 (C-15), 131.2 (C-5), 131.0 (C-4), 130.6 (C-3), 129.8 (C-13), 129.6 (C-6), 129.3 (C-1), 128.0 (C-9), 127.0 (C-12), 125.9 (C-10), 125.9 (C-2), 125.4 (C-8), 123.2 (C-14), 122.4 (C-16), 122.4 (C-7), 119.8(C-16), 35.4 (C-17), 32.1 (C-18) ppm;
MS (ASAP): m/z = 336.9 (100%, $[M]^{+}$).

7-*tert*-Butylpyrenylboronic acid pinacol ester (9)
Under argon atmosphere, compound **8** (3.0 g, 8.9 mmol) was dissolved in THF (100 mL), and cooled to -78°C. Then under stirring *n*-BuLi (2.5 M in hexane, 6.4 mL, 16 mmol) was added dropwise, stirring was continued for 2 h, 2-isopropoxy-4,4,5,5-tetramethyl-1,3,2-dioxaborolane (3.63 mL, 16 mmol) was added dropwise, and the reaction mixture was allowed to warm to RT. The reaction was stirred overnight, quenched with HCl (1 M, 20 mL), the organic phase separated, and the aqueous phase extracted with DCM (3 × 20 mL). The combined organic phases were washed with water (50 mL), brine (50 mL), and dried over $MgSO_4$. The solvent was evaporated under reduced pressure, and compound **9** (2.87 g, 84%, [942506-80-1]) was obtained after column chromatography (SiO_2 + 5% boric acid, petroleum ether/DCM, 9:1); m.p. 178°C; R_F = 0.11 (petroleum ether/DCM, 9:1);
IR (KBr): $\tilde{\nu}$ = 2960*s*, 1601*m*, 1508*m*, 1460*w*, 1419*w*, 1388*s*, 1375*s*, 1352*s*, 1310*s*, 1282*m*, 1226*m*, 1144*s*, 1110*m*, 1038*m*, 962*w*,877*s*, 851*s*, 815*w*, 728*w*, 690*s*, 674*m* cm^{-1};
UV/vis ($CHCl_3$): λ_{max} (log ε) = 250 (4.25), 272 (3.9), 283 (4.06), 338 (3.99), 354 (4.13), 382 (3.14) nm;
^{1}H NMR (400 MHz, $CDCl_3$): δ = 9.04 (d, *J* = 9.2 Hz, 1H, 2-H), 8.51 (d, *J* = 7.7 Hz, 1H, 12-H), 8.25 (d, *J* = 1.8 Hz, 1H, 16-H), 8.23 (d, *J* = 1.6 Hz, 1H, 14-H), 8.13 (d, *J* = 7.7 Hz, 1H, 13-H), 8.12 (d, *J* = 7.7 Hz, 1H, 2-H), 8.10 (d, *J* = 7.7 Hz, 1H, 9), 8.04 (d, *J* = 8.9 Hz, 1H, 8-H), 1.60 (s, 9H, 18-H_3), 1.50 (s, 12H, 20-H_3) ppm;
^{13}C NMR (101 MHz, $CDCl_3$): δ = 148.8 (C-15), 136.3 (C-3), 133.5 (C-12), 133.3 (C-7), 131.0 (C-4), 130.6 (C-5), 128.7 C-9), 127.9 (C-2), 127.9 (C-1), 127.3 (C-8), 124.3 (C-11), 123.8 (C-13), 122.8 (C6, C-10), 122.5 (C-14), 122.5 (C-16), 83.8 (C-19), 35.2 (C-17), 31.9 (C-18), 25.1 (C-20) ppm;
MS (ASAP): m/z = 385.0 (100%, $[M]^{+}$).

Tetraphenylthene (10)
Under an argon atmosphere, zinc powder (30 g,495 mmol) was suspended in THF (150 mL), the mixture was cooled to -40°C, and $TiCl_4$ (25 mL, 228 mmol) was added dropwise. The reaction was allowed to warm to RT and stirred under reflux for 2h. Then the mixture was cooled down 0°C, benzophenone (2.0 g, 126 mmol) was added, and the mixture was heated under reflux overnight. The mixture was cooled to RT, a saturated potassium carbonate solution (400 mL) was added, and the precipitate was collected and air-dried overnight. Finally, the solid was dissolved in DCM (200 mL), the mixture was filtered, and the solvent of the filtrate was removed under reduced pressure to obtain a white solid, which was washed with cold EtOH and dried to yield **10** (18.8 g, 90%, [632-51-9]) as a white powder; m.p. 222.3°C; ^{1}H NMR (400 MHz, $CDCl_3$): δ = 7.14 – 7.09 (m, 12H), 7.07 – 7.03 (m, 8H) ppm.

Tetrakis(4-bromophenyl)ethene (11)
To a mixture of compound **10** (1.0 g, 3 mmol), $FeCl_3$ (24 mg, 0.15 mmol) in $CHCl_3$ (15 mL) was added Br_2 (0.63 mL, 12.3 mmol) at 0°C in the dark. The reaction was stirred at RT for 3 h and quenched carefully with cyclohexene (1.2 mL, 12.3 mmol). The mixture was stirred for 1 h, poured into water (30 mL), filtered off the residue, and the organic phase separated. The aqueous phase was extracted with DCM (30 mL), and the combined organic phases were dried over $MgSO_4$. Once the solvent was removed under reduced pressure, the solid and the precipitate were washed with cold EtOH (30 mL) to obtain **11** (1.85 g, 95%, [1341195-20-7]). ^{1}H NMR (400 MHz, $CDCl_3$):
δ = 7.26 (dd, *J* = 8.5, 1.9 Hz, 8H), 6.59 (dd, *J* = 8.5, 1.8 Hz, 8H) ppm.

Tetrakis(4-(7-(*tert*-butyl)pyrenyl)phenyl)ethene (12)
Compound **11** (0.5 g, 0.77 mmol), **9** (1.33 g, 3.5 mmol), and potassium carbonate (1.07 g, 7.7 mmol) were dissolved in toluene/H_2O (2:1, 30 mL) under argon atmosphere, and the reaction mixture was degassed. Subsequently P(t-Bu)$_3$ (0.04 mL, 0.15 mmol) and $Pd(OAc)_2$ (8 mg, 0.04 mmol) were added, and the mixture was stirred under reflux for 33 h. The reaction was then quenched with HCl (0.3 M, 10 mL), and the organic phase was separated. The aqueous phase was extracted with DCM (3 × 50 mL), the combined organic phases were washed with water (50 mL), brine (50 mL), and dried over $MgSO_4$. Once the solvent was evaporated under reduced pressure, the solid was purified by column chromatography (SiO_2, petroleum ether/DCM, 9:1 → 3:1) and recrystallized from $CHCl_3$ to obtain **12** (154 mg, 15%) as a yellow solid; m.p. >330°C; R_F = 0.13 (petroleum ether/DCM, 3:1);
IR (KBr): $\tilde{\nu}$ = 2962*w*, 1636*br*, 1384*s*, 877*w* cm^{-1};
UV/vis ($CHCl_3$): λ_{max} (log ε) = 249 (4.15), 274 (3.8), 284 (3.95), 352 (4.06) nm;
^{1}H NMR (500 MHz, $CDCl_3$): δ = 8.25 – 8.20 (m, 12H, 7-H + 18-H + 21-H), 8.09 (s, 8H, 17-H, 12-H), 8.05

(d, *J* = 7.8 Hz, 4H, 8-H), 8.01 (d, *J* = 2.4 Hz, 4H, 19-H), 7.82 (d, *J* = 9.4 Hz, 4H, 13-H), 7.61 (m, 8H, 3-H), 7.56 (m, 8H, 4-H), 1.56 (s, 36H, 22-H_3) ppm;
^{13}C NMR (126 MHz, $CDCl_3$): δ = 149.2 (C-20), 142.8 (C-1), 141.8 (C-2), 139.9 (C-6), 137.5 (C-5), 131.8 (C-4), 131.5 (C-16), 131.0 (C-11), 130.6 (C-9), 130.3 (C-3), 128.5 (C-10), 127.9 (C-13), 127.8 (C-12), 127.4 (C-17), 125.3 (C-7), 125.1 (C-14), 124.6 (C-18), 123.3 (C-15), 122.5 (C-19), 122.2 (C-1), 35.3 (C-22), 32.1 (C-23) ppm;
MS (ESI): m/z = 1357.67 (100%, $[M]^{+}$).

2-(4-Bromophenyl)benzo[*b*]thiophene (13)
2-Benzothienylboronic acid (5 g, 28.1 mmol), 4-bromo-1-iodobenzene (7.95 g, 28.1 mmol), and potassium carbonate (11.65 g, 84.3 mmol) were dissolved in toluene (200 mL) under argon atmosphere, and the mixture was degassed. Subsequently $P(t\text{-}Bu)_3$ (0.27 mL, 1.1 mmol) and $Pd(OAc)_2$ (63 mg, 0.3 mmol) were added, and the reaction was stirred under reflux for 10 h. Water (50 mL) was added to the reaction, and the organic phase was separated. The aqueous phase was extracted with DCM (3 × 50 mL), the combined organic phases were washed with brine (50 mL) and dried over $MgSO_4$. Once the solvent was evaporated under reduced pressure, the solid was purified by column chromatography (SiO_2, toluene) to obtain **13** (6.47 g, 69%, [19437-86-6]) as white flakes; m.p. 207 °C (lit.:[36] 205°C); R_F = 0.41 (petroleum ether/DCM, 9:1);
IR (KBr): $\tilde{\nu}$ = 1636*br*, 1484*w*, 1432*w*, 1384*w*, 1076*w*, 1007*w*, 940*w*, 814*s*, 744*m*, 727*m*, 539*w*, 475*m* cm^{-1};
UV/vis ($CHCl_3$): λ_{max} (log ε) = 236 (4.17), 259 (4.03), 302 (4.41) nm;
^{1}H NMR (400 MHz, THF-d_8): δ = 9.72–9.68 (m, 1H, 1-H), 9.63 (m, 1H, 4-H), 9.56 (s, 1H, 7-H), 9.54 – 9.51 (m, 2H, 11-H), 9.46 – 9.41 (m, 2H, 10-H), 9.21 – 9.12 (m, 2H, 3-H + 2-H) ppm;
^{13}C NMR (101 MHz, THF-d_8): δ = 143.6 (C-9), 142.0 (C-5), 140.6 (C-6), 134.6 (C-8), 133.1 (C-10), 128.9 (C-10), 125.7 (C-3), 125.6 (C-2), 124.7 (C-4), 123.2 (C-1), 123.0 (C-12), 121.4 (C-11) ppm;
MS (ASAP): m/z = 290.8 (100%, $[M]^{+}$).

4-(Benzo[*b*]thiophen-2-yl)phenylboronic acid pinacol ester (14)
Under argon atmosphere, compound **13** (6 g, 17.8 mmol) was dissolved in THF (200 mL), and cooled to -78°C. Then under stirring, *n*-BuLi (2.5 M in hexane, 12.8 mL, 32 mmol) was added dropwise, stirring was continued for 2 h, 2-isopropoxy-4,4,5,5-tetramethyl-1,3,2-dioxaborolane (8 mL, 39 mmol) was added dropwise, and the reaction mixture was allowed to warm to RT. The reaction was stirred overnight, quenched with HCl (1 M, 40 mL), the organic phase separated, and the aqueous phase extracted with DCM (3 × 50 mL). The combined organic phases were washed with water (50 mL), brine (50 mL), and dried over $MgSO_4$. The solvent was evaporated under reduced pressure, and compound **13** (4.36 g, 72%, [1394004-97-7]) was obtained as colorless needles from column chromatography (SiO_2 + 5% boric acid, petroleum ether/DCM, 9:1); m.p. 170°C; R_F = 0.50 (petroleum ether/DCM, 9:1);
IR (KBr): $\tilde{\nu}$ = 3056*w*, 2977*m*, 1608*m*, 1501*w*, 1458*w*, 1435*w*, 1400*s*,1362*s*, 1327*m*, 1300*w*, 1270*w*, 1212*w*, 1193*w*, 1142*s*, 1106*w*, 1094*s*, 1018*w*, 962*w*, 942*w*, 858*m*, 820*s*, 748*m*, 724*m*, 671*w*, 654*m*, 576*w*, 443*w* cm^{-1};
UV/vis ($CHCl_3$): λ_{max} (log ε) = 237 (3.93), 261 (3.79), 309 (4.18), 317 (4.19) nm;
^{1}H NMR (400 MHz, $CDCl_3$): δ = 7.89 – 7.86 (m, 2H, 10-H), 7.85 – 7.82 (m, 1H, 1-H), 7.80 – 7.76 (m, 1H, 4-H), 7.75 – 7.71 (m, 2H, 11-H), 7.62 (s, 1H, 7-H), 7.38 – 7.29 (m, 2H, 3-H + 2-H), 1.37 (s, 12H, 14-H_3) ppm;
^{13}C NMR (101 MHz, $CDCl_3$): δ = 144.2 (C-9), 140.8 (C-5), 139.8 (C-6), 136.9 (C-8), 135.5 (C-10), 129.1 (C-13), 125.8 (C-10), 124.7 (C-3), 124.6 (C-2), 123.8 (C-4), 122.4 (C-1), 120.2 (C-7), 84.1 (C-13), 25.0 (C-14) ppm;
MS (ASAP): m/z = 337.8 (100%, $[M]^{+}$).

2-Iodobiphenyl (15)
2-Aminobiphenyl (2.53 g, 15 mmol) was suspended in water (15 mL) and conc. HCl (3 mL) was added dropwise under stirring. The reaction mixture was cooled to 0°C, and a solution of sodium nitrite (1.17 g, 17 mmol) in water (5 mL) was added dropwise. The reaction temperature was carefully monitored to be less than 5°C. Subsequently, the reaction mixture was stirred at 0°C for 45 min, turned yellow, and an aqueous solution of potassium iodide (4.90 g, 30 mmol, 50 mL), was added dropwise at 0°C. Then the reaction was allowed to warm to RT, stirred overnight, and extracted with Et_2O (4 × 100 mL). The combined organic phases were washed with HCl (3 M, 3 × 10 mL), saturated sodium bicarbonate solution (2 ×20 mL), brine (2 ×20 mL), and dried over $MgSO_4$. The solvent was evaporated under reduced pressure to obtain a reddish oil that was subjected to distillation (120°C, 0.06 mbar), and **15** (3 g,71.4%, [20442-79-9]) was obtained as a colorless liquid; b.p. 120°C/0.06 mbar (lit.: [37] 130-134°C (at 5 mbar);
IR (KBr): $\tilde{\nu}$ = 3057*m*, 2360*w*, 1950*w*, 1806*w*, 1579*w*, 1556*w*, 1496*w*, 1460*s*, 1444*m*, 1427*m*, 1415*m*, 1017*s*, 1004*s*, 769*m*, 747*s*, 699*s* cm^{-1};
^{1}H NMR (400 MHz, $CDCl_3$): δ = 7.99 (d, *J* = 7.9 Hz, 1H, 3-H), 7.49−7.31 (m, 7H, 5-H + 6-H + 8-H + 9-H + 10-H + 11-H + 12-H), 7.06 (td, *J* = 7.8, 1.5 Hz, 1H, 4-H) ppm;
^{13}C NMR (101 MHz, $CDCl_3$): δ = 146.7 (C-1), 144.3 (C-7), 139.6 (C3), 130.2 (C6), 129.4 (C-9 + C-11), 128.9 (C-4), 128.2 (C-5), 128.1 (C-8, C-12), 127.7 (C-10), 98.8 (C-2) ppm;
MS (API, DMF): found m/z = 279.9750 (100%, $[M]^{+}$), calcd for $C_{12}H_9I$ m/z = 279.9743.

9-(2-Biphenyl)-9-fluorenol (16)
Compound **15** (4 g, 14.3 mmol) was dissolved in Et_2O (40 mL) under argon atmosphere, cooled to -78°C, and under rigorously stirring *t*-BuLi (1.7 M, 18.5 mL,

31.4 mmol) was added dropwise. The reaction mixture was stirred at -78°C for 1 h, fluorenone (2.57 g, 14.3 mmol), dissolved in Et_2O (50 mL), was added dropwise, and stirred for 45 min. Afterward, the reaction mixture was allowed to warm to RT, poured into water (50 mL), extracted with Et_2O (3 × 100 mL), and dried over $MgSO_4$. Finally, the solvent was removed under reduced pressure, and the resulting solid was washed with cold EtOH to obtain **16** (4.14 g, 87%, [67665-44-5]) as a white powder; m.p. 168°C; R_F = 0.41 (hexane/EE, 6:1);
IR (KBr): $\tilde{\nu}$ = 3531*s*, 3055*w*, 1474*m*, 1447*s*, 1344*s*, 1287*w*, 1166*m*, 1114*w*, 1019*m*, 912*m*, 759*s*, 770*s*, 745s, 732*s*, 702*s*, 639*s*, 554*m* cm^{-1};
^{1}H NMR (500 MHz, $CDCl_3$): δ = 8.47 (dd, *J* = 8.0, 1.0 Hz, 1H, 3-H), 7.54 (td, *J* = 7.7, 1.5 Hz, 1H, 4-H), 7.32 (td, *J* = 7.4, 1.4 Hz, 1H, 5-H), 7.23–7.13 (m, 8H, 14-H + 15-H + 16-H + 17-H + 18-H + 19-H + 20-H + 21-H), 6.91 (dd, *J* = 7.5, 1.4 Hz, 1H, 6-H), 6.86−6.80 (m, 1H, 10-H), 6.62 (t, *J* = 7.7 Hz, 2H, 9-H + 11-H), 6.01 (dd, *J* = 8.2, 1.2 Hz, 2H, 8-H + 12-H), 2.25 (s, 1H, 13-OH) ppm;
^{13}C NMR (125 MHz, $CDCl_3$): δ = 150.7 (C-13a + C-21a), 141.1 (C-1), 140.5 (C-7), 140.3 (C17a + C-17b), 139.8 (C-2), 131.4 (C-6), 129.0 (C-8 + C-12), 128.8 (C-19 + C-16), 128.0 (C-15 + C-20), 127.3 (C-4), 127.0 (C-5), 126.4 (C-3), 126.2 (C-9 + C-11), 125.2 (C-10), 124.5 (C-14 + C-21), 120.2 (C-17 + C-18), 82.6 (C-13) ppm;
MS (API, DMF): found m/z = 334.1358 (100%, $[M]^{+\cdot}$), calcd for $C_{25}H_{18}O$ m/z = 334.1352.

9,9´−Spirobifluorene (17)
Compound **16** (5 g, 15 mmol) was suspended in conc. acetic acid (45 mL) and stirred under reflux. Once the reaction was refluxing, conc. HCL (0.05 mL) was added, and stirring was continued at reflux for 30 min. Subsequently, the reaction was cooled, was poured into water (50 mL), filtrated, and the precipitate was air-dried to obtain **17** (4.47 g, 95%, [159-66-0]) as colorless powder; m.p. 203°C (lit.:[38] 204 °C);
IR (KBr): $\tilde{\nu}$ = 3060*w*, 1601*w*, 1472*w*, 1445*m*, 1208*w*, 1152*w*, 1102*w*, 1029*w*, 858*w*, 749*s*, 727*s*, 632*m*, 413*m* cm^{-1};
^{1}H NMR (400 MHz, $CDCl_3$): δ = 7.89 (d, *J* = 7.6 Hz, 4H, 4-H + 4‘-H + 5-H + 5‘-H), 7.40 (t, *J* = 7.4 Hz, 4H, 3-H + 3‘-H + 6-H + 6‘-H), 7.14 (t, *J* = 7.4 Hz, 4H, 2-H + 2‘-H + 7-H + 7‘-H), 6.78 (d, *J* = 7.6 Hz, 4H, 1-H + 1‘-H + 8-H + 8‘-H) ppm;
^{13}C NMR (100 MHz, $CDCl_3$): δ = 148.9 (C-8a +C-8a‘ + C-9a + C-9a‘), 141.9 (C-4a + C-4a‘ + C-4b + C-4b‘), 127.9 (C-3 + C-3‘ + C-6 + C-6‘), 127.8 (C-2 + C-2‘ + C-7 + C-7‘), 124.2 (C-1 + C-1 + C-8 + C-8‘), 120.1 (C-4 + C-4‘ + C-5 + C-5‘), 66.1 (C-9) ppm;
MS (API, DMF): found m/z = 316.3946 (100%, $[M]^{+\cdot}$), calcd for $C_{25}H_{16}$ m/z = 316.3940.

2,2´,7,7´−Tetrabromo-9,9´-spirobifluorene (18)
Compound **17** (1 g, 3.16 mmol) was suspended in $CHCl_3$ (10 mL) under stirring. Fe(III)Cl_3 × 6 H_2O (26 mg, 0.1 mmol) and Br_2 (0.67 mL, 13 mmol) were added at 0°C, stirred at RT for 3 h, the mixture was quenched with cyclohexene (1.3 mL, 13 mmol), again stirred for 1 h, poured into water (25 mL), extracted with DCM (3 × 50 mL), and dried over $MgSO_4$. After removing most of the solvent *in vacuo*, the mixture was precipitated with cold EtOH, and the precipitate was washed with cold EtOH (3 × 5 mL) to obtain **18** (1.8 g, 90%, [128055-74-3]) after air-drying; m.p. >300°C (lit.:[39] >320 °C); R_F = 0.8 (hexane/ethyl acetate, 6:1);
IR (KBr): $\tilde{\nu}$ = 1594*m*, 1571*m*, 1450*s*, 1410*m*, 1395*m*, 1248*m*, 1167*m*, 1125*w*, 1005*m*, 949*m*, 876*w*, 805*s*, 730*s*, 670*m*, 507*m*, 422*m* cm^{-1};
^{1}H NMR (400 MHz, $CDCl_3$): δ = 7.71–7.66 (m, 4H, 4-H + 4‘-H + 5-H + 5‘-H), 7.54 (dd, *J* = 8.2, 1.8 Hz, 4H, 3-H + 3‘-H + 6-H + 6‘-H), 6.84–6.83 (m, 4H, 1-H + 1‘-H + 8-H + 8‘-H) ppm;
^{13}C NMR (100 MHz, $CDCl_3$): δ = 149.0 (C-8a + C-8a‘ + C-9a + C-9a‘), 139.7 (C4a + C-4a‘ + C-4b + C-4b‘), 132.0 (C-3 + C-3‘ + C-6 + C-6‘), 127.5 (C-1 + C-1‘ + C-8 + C-8‘), 122.3 (C-2 + C-2‘ + C-7 + C-7‘), 121.8 (C-4 + C-4‘ + C-5 + C-5‘), 65.3 (C-9) ppm;
MS (API, DMF): found m/z = 627.7673 (100%, $[M]^{+\cdot}$), calcd for $C_{25}H_{12}Br_4$ m/z = 627.7667.

2,2',7,7'-Tetrakis(4-(benzo[b]thiophen-2-yl)phenyl)-9,9'-spirobifluorene (19)
Compound **18** (0.5 g, 0.79 mmol), **14** (1.46 g, 4.3 mmol), and potassium carbonate (1.09 g, 7.9 mmol) were dissolved in toluene/H_2O (2:1, 30 mL) under argon atmosphere and degassed multiple times. Subsequently P(t-Bu)$_3$ (0.04 mL, 0.15 mmol) and $Pd(OAc)_2$ (8 mg, 0.04 mmol) were added and the reaction was stirred under reflux for 38 h. The reaction was then quenched with HCl (0.3 M, 10 mL) and the organic phase was separated. The aqueous phase was extracted with DCM (3 × 50 mL), the combined organic phases were washed with water (50 mL), brine (50 mL), and dried over $MgSO_4$. Once the solvent was evaporated under reduced pressure, the solid was dissolved in hot $CHCl_3$ and precipitated by adding the solution dropwise into cold EtOH to obtain **12** (232 mg, 23%) as a yellow solid after filtrating and air-drying; m.p. 271.4°C; R_F = 0.11 (petroleum ether/DCM, 3:1);
IR (KBr): $\tilde{\nu}$ = 1636*br*, 1467*w*, 812*w* cm^{-1};
UV/vis ($CHCl_3$): λ_{max} (log ε) = 234 (4.14), 263 (3.94), 288 (3.97), 360 (4.5) nm;
^{1}H NMR (500 MHz, $CDCl_3$): δ = 8.00 – 7.97 (d, *J* = 8.0 Hz, 4H, 4-H), 7.79 – 7.75 (m, 4H, 16-H), 7.73–7.71 (m, 4H, 19-H), 7.71 – 7.69 (m, 4H, 5-H), 7.64 (m, 8H, 9-H), 7.51 (m, 8H, 10-H), 7.48 (d, *J* = 1.0 Hz, 4H, 13-H), 7.30 (ddd, *J* = 7.9, 7.1, 1.3 Hz, 4H, 18-H), 7.26 (ddd, *J* = 8.3, 7.1, 1.4 Hz, 4H, 17-H), 7.08 (d, *J* = 1.3 Hz, 4H, 7-H) ppm;
^{13}C NMR (126 MHz, $CDCl_3$): δ = 150.0 (C-2), 143.9 (C-6), 141.1 (C-3), 140.8 (C-14), 140.8 (C-11), 140.5 (C-8), 139.6 (C-15), 133.4 (C-12), 127.7 (C-10), 127.2 (C-5), 126.9 (C-9), 124.7 (C-18), 124.5 (C-17), 123.7 (C-19), 122.8 (C-7), 122.4 (C-16), 120.8 (C-4), 119.6 (C-13), 66.3 (C-1) ppm.

2,2',7,7'-Tetrakis(4-(7-(*tert*-butyl)pyrenyl)-9,9'-spirobifluorene (20)

Compound **18** (0.5 g, 0.79 mmol), **9** (1.09 g, 7.9 mmol), and potassium carbonate (1.09 g, 7.9 mmol) were dissolved in toluene/H_2O (2:1, 30 mL) under argon atmosphere and degassed multiple times. Subsequently P(t-Bu)$_3$ (0.04 mL, 0.15 mmol) and $Pd(OAc)_2$ (8 mg, 0.04 mmol) were added, and the reaction was stirred under reflux for 31 h. Afterwards **9** (0.2 g, 0.5 mmol) and potassium carbonate (0.2 g, 1.4 mmol) were added, and the reaction mixture was stirred under reflux for another 14 h. The reaction was then quenched with HCl (0.3 M, 10 mL) and the organic phase was separated. The aqueous phase was extracted with DCM (3 × 50 mL), the combined organic phases were washed with water (50 mL), brine (50 mL), and dried over $MgSO_4$. After gradient column chromatography (petroleum ether /DCM, 9:1 → 3:1) and multiple recrystallizations from a $CHCl_3$/EtOH-mixture, **20** (212 mg, 20%, [669077-77-4]) was obtained as a yellow solid; m.p. >300°C; R_F = 0.06 (petroleum ether/DCM, 9:1);
IR (KBr): $\tilde{\nu}$ = 674*w*, 702*w*, 726*w*, 842*w*, 876*w*, 1156*vw*, 1226*w*, 1360*w*, 1384*w*, 1412*vw*, 1462*w*, 1638*br*, 1712*w*, 2366*w*, 2866*w*, 2902*w*, 2960*m*, 3048*w* cm^{-1};
UV/vis ($CHCl_3$): λ_{max} (log ε) = 248 (4.05), 275 (4), 283 (4.05), 362 (3.9) nm;
^{1}H NMR (500 MHz, $CDCl_3$): δ = 8.23 (*d*, *J* = 1.8 Hz, 4H, 23-H), 8.21 – 8.15 (*m*, 12H, 21-H + 15-H + 10-H), 8.06 (*s*, 8H, 19-H, 14-H), 8.04 (*d*, *J* = 7.6 Hz, 4H, 4-H), 7.98 (*d*, *J* = 7.8 Hz, 9-H), 7.96 (*d*, *J* = 9.2 Hz, 4H, 20-H), 7.73 (*dd*, *J* = 7.8, 1.6 Hz, 4H, 5-H), 7.43 (*s*, 4H, 7-H), 1.60 (*s*, 36H, 25-H$_3$) ppm;
^{13}C NMR (126 MHz, $CDCl_3$): δ = 149.5 (C-2), 149.3 (C-22), 141.2 (C-6), 140.9 (C-3), 137.7 (C-8), 131.5 (C-16), 131.0 (C-18), 130.7 (C-5), 130.6 (C-11), 128.4 (C-13), 127.9 (C-19), 127.7 (C-15), 127.4 (C-23), 127.4 (C-9), 126.7 (C-7), 125.2 (C-21), 125.1 (C-12), 124.6 (C-10), 123.3 (C-17), 122.6 (C-20), 122.2 (C-14), 120.4 (C-4), 66.5 (C-1), 35.4 (C-24), 32.1 (C-25) ppm;
MS (ESI, DCM): m/z = 1342.47 (100%, $[M]^{+}$).

2,7-Dibromofluorene (22)

Compound **21** (1 g**,** 6.02 mmol) was dissolved in $CHCl_3$, cooled to 0°C, and $FeBr_3$ (26 mg, 0.1 mmol) was added. In the dark and under stirring, Br_2 (0.93 mL, 18 mmol) was added. Stirring was continued for 3 h at RT, and subsequently cyclohexene (1.83 mL, 18 mmol) was added. After stirring the mixture for 1 h, water (30 mL) was added and the precipitate was filtered off, the organic phase separated, and the aqueous phase extracted with DCM (30 mL). The combined organic phases were dried over $MgSO_4$, the solvent was removed under reduced pressure, and the solid was combined with the previously precipitated solid. Finally, the solid was washed with cold EtOH (3 × 10 mL) to yield **21** (1.76 g, 89%, [16433-88-8]) as a colorless powder; m.p. 155°C (lit.:[40] 156-160°C); R_F = 0.9 (hexane/ethyl acetate, 3:1);
IR (KBr): $\tilde{\nu}$ = 3448*s*, 1580*w*, 1453*m*, 1392*m*, 1290*w*, 1272*w*, 1158*m*, 1054*m*, 1004*w*, 834*w*, 810*s*, 685*w*, 419*w* cm^{-1};
UV/vis ($CHCl_3$): λ_{max} (log ε) = 303 (4.22), 326 (4.11), 339 (4.02) nm;
^{1}H NMR (400 MHz, $CDCl_3$): δ = 7.64 (d, *J* = 0.9 Hz, 2H, 4-H + 5-H), 7.57 (d, *J* = 8.1 Hz, 2H, 3-H + 6-H), 7.49 (m, 2H, 1-H + 8-H), 3.82 (s, 2H, 9-H) ppm;
^{13}C NMR (100 MHz, $CDCl_3$): δ = 144.8 (C-9a + C-8a), 139.7 (C-4a + C-4b), 130.1 (C-3 + C-6), 128.3 (C-1 + C-8), 121.2 (C-4 + C-5), 120.9 (C-2 + C-7), 36.5 (C-9) ppm;
MS (APCI, positive): m/z = 321.8 (16%, $[M]^{+}$).

***N*^{2},*N*^{2},*N*^{7},*N*^{7}-Tetrakis(4-methoxyphenyl)fluorene-2,7-diamine (23)**

Compound **23** was obtained by reacting **22** (486 g, 1.6 mmol) and *t*-BuONa (0.36 g, 3.75 mmol) using GP1. After refluxing the reaction mixture under stirring overnight., the mixture was controlled by TLC, water (20 mL) was added, extracted with ethyl acetate (2 × 50 mL), the combined organic phases were dried over $MgSO_4$, and the solvent was evaporated under reduced pressure. After column chromatography (SiO_2, hexane/ethyl acetate, 3:1), **22** (473 mg, 78%, [1649427-53-1]) was obtained as a yellow solid; m.p. 76°C; R_F = 0.7 (hexane/ethyl acetate, 3:1);
IR (KBr): $\tilde{\nu}$ = 3447*s*, 2831*w*, 1612*w*, 1505*s*, 1466*m*, 1321*w*, 1269*w*, 1239*s*, 1179*w*, 1120*w*, 1035*w*, 827*w*, 594*w* cm^{-1};
UV/vis ($CHCl_3$): λ_{max} (log ε) = 264 (3.96), 343 (4.39), 385 (4.47), 409 (4.52) nm;
^{1}H NMR (400 MHz, DMSO-d6): δ = 7.50 (d, *J* = 8.3 Hz, 2H, 4-H + 5-H), 6.96 (d, *J* = 9 Hz, 8H, 12-H), 6.91 (d, 2H, 1-H + 8-H), 6.87 (d, *J* = 9.0 Hz, 8H, 11-H) 6.78 (dd, *J* = 8.3, 2.1 Hz, 2H, 3-H + 6-H), 3.71 (s, 12H, 13-H), 3.63 (s, 2H, 9-H) ppm;
^{13}C NMR (100 MHz, $CDCl_3$): δ = 155.7 (C-13), 147.1 (C-2 + C-7), 144.4 (C-9a + C-8a), 141.2 (C-10), 134.8 (C-4a + C-4b), 126.5 (C-12), 120.1 (C-4 + C-5) 120.0 (C-3 + C-6), 117.7 (C-1 + C-8), 115.3 (C-11), 55.7 (C-14), 36.8 (C-9) ppm;
MS (ESI, CH_2Cl_2): m/z = 620.3 (16%, $[M]^{+}$).

Acknowledgments

We would like to thank the late Dr. R Kluge for measuring the MS spectra and Dr. D. Ströhl, Y. Schiller, and S. Ludwig for the NMR spectra. Many thanks are also due to Mrs. V. Simon for measuring the IR and UV/vis spectra. Furthermore, we would like to thank M. Weiß and P. Palme for their valuable help in synthesizing some compounds. Finally, Dr. T. Kohlmann performed fluorescence spectra and lifetime measurements. Financial support by the European Regional Development Fund, EFRE (Project "Nanoscience", number W26000256) is gratefully acknowledged.

References

1- A. Kojima, K. Teshima, Y. Shirai, T. Miyasaka, Organometal Halide Perovskites as Visible-Light Sensitizers for Photovoltaic Cells, J. Am. Chem. Soc., **2009**, 131, 6050-6051.
2- https://www.nrel.gov/pv/assets/pdfs/best-research-cell-efficiencies-rev220126.pdf (last accessed 2022, March 28th).
3- M. Kim, J. Jeong, H.Z. Lu, T.K. Lee, F.T. Eickemeyer, Y.H. Liu, I.W. Choi, S.J. Choi, Y. Jo, H.B. Kim, S.I. Mo, Y. K. Kim, H. Lee, N.G. An, S. Cho, W.R. Tress, S.M. Zakeeruddin, A. Hagfeldt, J.Y. Kim, M. Gratzel, D.S. Kim, Conformal quantum dot-SnO_2 layers as electron transporters for efficient perovskite solar cells, Science, **2022**, 375, 302-306.
4- P. Mahajan, R. Datt, W.C. Tsoi, V. Gupta, A. Tomar, S. Arya, Recent progress, fabrication challenges and stability issues of lead-free tin-based perovskite thin films in the field of photovoltaics, Coord. Chem. Rev., **2021**, 429, 213633.
5- R. Kour, S. Arya, S. Verma, J. Gupta, P. Bandhoria, R. Datt, V. Gupta, Potential substitutes for replacement of lead in perovskite solar cells: a review, Glob. Chall., **2019**, 3, 1900059.
6- X.X. Yin, Z.N. Song, Z. F. Li, W.H. Tang, Toward ideal hole transport materials: a review on recent progress in dopant-free hole transport materials for fabricating efficient and stable perovskite solar cells, Energy. Environ. Sci., **2020**, 13, 4057-4086.
7- A. Urbina, The balance between efficiency, stability and environmental impacts in perovskite solar cells: a review, J. Phys. Energy, **2020**, 2, 022001.
8- D.Y. Li, D.Y. Zhang, K.S. Lim, Y. Hu, Y.G. Rong, A.Y. Mei, N.G. Park, H.W. Han, A Review on Scaling Up Perovskite Solar Cells, Adv. Funct. Mater, **2021**, 31.
9- https://abcr.com/de_en/ab287840, (last accessed: 2022, March 28th).
10- P. Mahajan, B. Padha, V. Gupta, R. Datt. W.C. Tsoi, S. Datapathi, S. Arya, Review of current progress in hole-transportin materials for perovskite solar cells, J. Energ. Chem., **2022**, 68, 333-386.
11- F.M. Rombach, S.A. Haque, T.J. Macdonald, Lessons learned from spiro-OMeTAD and PTAA in perovskite solar cells, Energy. Environ. Sci., **2021**, 14, 5161-5190.
12- T.P. Osedach, T.L. Andrew, V. Bulovic, Effect of synthetic accessibility on the commercial viability of organic photovoltaics, Energy. Environ. Sci., **2013**, 6, 711-718.
13- C. Lambert, G. Noll, One- and two-dimensional electron transfer processes in triarylamines with multiple redox centers, Angew. Chem. Int. Edit., **1998**, 37, 2107-2110.
14- Y. Liu, C. Tao, G.H. Xie, J. Van der Velden, S. Marras, Z.H. Luo, X. Zeng, A. Petrozza, C.L. Yang, Hexa-substituted benzene derivatives as hole-transporting materials for efficient perovskite solar cells, Dyes Pigments, **2019**, 163, 267-273.
15- H.D. Zhao, C. Tanjutco, S. Thayumanavan, Design and synthesis of stable triarylamines for hole-transport applications, Tetrahedron Lett., **2001**, 42, 4421-4424.
16- C.I. Schilling, O. Plietzsch, M. Nieger, T. Muller, S. Brase, Fourfold Suzuki-Miyaura and Sonogashira Cross-Coupling Reactions on Tetrahedral Methane and Adamantane Derivatives, Eur. J. Org. Chem., **2011**, 1743-1754.
17- Q. D. Ou, C. Li, Q. K. Wang, Y.Q. Li, J.X. Tang, Recent Advances in Energetics of Metal Halide Perovskite Interfaces, Adv. Mater. Interfaces, **2017**, 4.
18- P. Schulz, E. Edri, S. Kirmayer, G. Hodes, D. Cahen, A. Kahn, Interface energetics in organo-metal halide perovskite-based photovoltaic cells, Energy. Environ. Sci., **2014**, 7, 1377-1381.
19- S.H. Wang, T. Sakurai, W.J. Wen, Y.B. Qi, Energy Level Alignment at Interfaces in Metal Halide Perovskite Solar Cells, Adv. Mater. Interfaces, **2018**, 5.
20- Y. Zhang, C. Kou, J.J. Zhang, Y.H. Liu, W.H. Li, Z.S. Bo, M. Shao, Crosslinked and dopant free hole transport materials for efficient and stable planar perovskite solar cells, J. Mater. Chem. A, **2019**, 7, 5522-5529.
21- W.J. Chi, Z.S. Li, The theoretical investigation on the 4-(4-phenyl-4-alpha-naphthylbutadieny)-triphenylamine derivatives as hole-transporting materials for perovskite-type solar cells, Phys. Chem. Chem. Phys., **2015**, 17, 5991-5998.
22- D.R.T. Zahn, G.N. Gavrila, M. Gorgoi, The transport gap of organic semiconductors studied using the combination of direct and inverse photoemission, Chem. Phys., **2006**, 325, 99-112.
23- J. Sworakowski, How accurate are energies of HOMO and LUMO levels in small-molecule organic semiconductors determined from cyclic voltammetry or optical spectroscopy?, Synthetic Met., **2018**, 235, 125-130.
24- J.C.S. Costa, R.J.S. Taveira, C.F.R.A.C. Lima, A. Mendes, L.M.N.B.F. Santos, Optical band gaps of organic semiconductor materials, Opt. Mater., **2016**, 58, 51-60.
25- N.G. Tsierkezos, Cyclic voltammetric studies of ferrocene in nonaqueous solvents in the temperature range from 248.15 to 298.15 K, J. Solution Chem., **2007**, 36, 289-302.
26- N.G. Connelly, W.E. Geiger, Chemical redox agents for organometallic chemistry, Chem. Rev., **1996**, 96, 877-910.
27- E.M. Espinoza, J.A. Clark, J. Soliman, J.B. Derr, M. Morales, V.I. Vullev, Practical Aspects of Cyclic Voltammetry: How to Estimate Reduction Potentials When Irreversibility Prevails,

J. Electrochem. Soc., **2019**, 166, H3175-H3187.
28- V.V. Pavlishchuk, A.W. Addison, Conversion constants for redox potentials measured versus different reference electrodes in acetonitrile solutions at 25 degrees C, Inorg. Chim. Acta, **2000**, 298, 97-102.
29- A.M. Bond, K.B. Oldham, G.A. Snook, Use of the ferrocene oxidation process to provide both reference electrode potential calibration and a simple measurement (via semiintegration) of the uncompensated resistance in cyclic voltammetric studies in high resistance organic solvents, Anal. Chem., **2000**, 72, 3492-3496.
30- C.G. Zoski, Handbook of Electrochemistry, 1st ed., Elsevier, Amsterdam, Boston, **2007**.
31- M.J. Frisch, G.W. Trucks, H.B. Schlegel, G.E. Scuseria, M.A. Robb, J.R. Cheeseman, G. Scalmani, V. Barone, G.A. Petersson, H. Nakatsuji, X. Li, M. Caricato, A.V. Marenich, J. Bloino, B.G. Janesko, R. Gomperts, B. Mennucci, H.P. Hratchian, J.V. Ortiz, A.F. Izmaylov, J.L. Sonnenberg, D. Williams-Young, F. Ding, F. Lipparini, F. Egidi, J. Goings, B. Peng, A. Petrone, T. Henderson, D. Ranasinghe, V.G. Zakrzewski, J. Gao, N. Rega, G. Zheng, W. Liang, M. Hada, M. Ehara, K. Toyota, R. Fukuda, J. Hasegawa, M. Ishida, T. Nakajima, Y. Honda, O. Kitao, H. Nakai, T. Vreven, K. Throssell, J.A. Montgomery, Jr., J.E. Peralta, F. Ogliaro, M.J. Bearpark, J.J. Heyd, E.N. Brothers, K.N. Kudin, V.N. Staroverov, T.A. Keith, R. Kobayashi, J. Normand, K. Raghavachari, A.P. Rendell, J.C. Burant, S.S. Iyengar, J. Tomasi, M. Cossi, J.M. Millam, M. Klene, C. Adamo, R. Cammi, J.W. Ochterski, R.L. Martin, K. Morokuma, O. Farkas, J.B. Foresman, D.J. Fox, Gaussian 16 Rev. C 01, **2016**.
32- S. Lei, A.V. Heyen, S. De Feyter, M. Surin, R. Lazzaroni, S. Rosenfeldt, M. Ballauff, P. Lindner, D. Mossinger, S. Hoger, Two-Dimensional Oligo(phenylene-ethynylene-butadiynylene)s: All-Covalent Nanoscale Spoked Wheels, Chem-Eur. J., **2009**, 15, 2518-2535.
33- M.J. Kim, S. Ahn, J. Yi, J.T. Hupp, J.M. Notestein, O.K. Farha, S.J. Lee, Ni(II) complex on a bispyridine-based porous organic polymer as a heterogeneous catalyst for ethylene oligomerization, Catal. Sci. Technol., **2017**, 7, 4351-4354.
34- M.C.C. Ng, J.B. Harper, A.P.J. Stampfl, G.J. Kearley, S. Rols, J.A. Stride, Central-Atom Size Effects on the Methyl Torsions of Group XIV Tetratolyls, Chem-Eur. J., **2012**, 18, 13018-13024.
35- T.M. Figueira-Duarte, S.C. Simon, M. Wagner, S.I. Drtezhinin, K.A. Zachariasse, K. Müllen, Polypyrene Dendrimers, Angew. Chem. Int. Edit., **2008**, 47, 10175-10178.
36- M.A. Zwijnenburg, G. Cheng, T.O. McDonald, K.E. Jelfs, J.X. Jiang, S.J. Ren, T. Hasell, F. Blanc, A.I. Cooper, D.J. Adams, Shedding Light on Structure-Property Relationships for Conjugated Microporous Polymers: The Importance of Rings and Strain, Macromolecules, **2013**, 46, 7696-7704.
37- E. Ibuki, S. Ozasa, K. Murai, Studies of Polyphenyls and Polyphenylenes .1. Syntheses and Infrared and Electronic-Spectra of Several Sexiphenyls, Bull. Chem. Soc. Jpn., **1975**, 48, 1868-1874.
38- C. Poriel, J.J. Liang, J. Rault-Berthelot, F. Barriere, N. Cocherel, A.M.Z. Slawin, D. Horhant, M. Virboul, G. Alcaraz, N. Audebrand, L. Vignau, N. Huby, G. Wantz, L. Hirsch, Dispirofluorene-indenofluorene derivatives as new building blocks for blue organic electroluminescent devices and electroactive polymers, Chem-Eur. J., **2007**, 13, 10055-10069.
39- W.F. Jiang, H.L. Wang, A.G. Wang, Z.Q. Li, Simple and efficient method for obtaining fluorene and spirobifluorene bromide derivatives, Synthetic Commun., **2008**, 38, 1888-1895.
40- H.H. Lu, Y.S. Ma, N. J. Yang, G.H. Lin, Y.C. Wu, S.A. Chen, Creating a Pseudometallic State of K+ by Intercalation into 18-Crown-6 Grafted on Polyfluorene as Electron Injection Layer for High-Performance PLEDs with Oxygen- and Moisture-Stable Al Cathode, J. Am. Chem. Soc., **2011**, 133, 9634-9637.